The role of anisotropy in the response of the titanium alloy Ti–6Al–4V to shock loading

Cite as: J. Appl. Phys. **104**, 073531 (2008); https://doi.org/10.1063/1.2991164
Submitted: 30 June 2008 . Accepted: 17 August 2008 . Published Online: 09 October 2008

J. C. F. Millett, G. Whiteman, N. K. Bourne, and G. T. Gray

The role of anisotropy in the response of the titanium alloy Ti–6Al–4V to shock loading

J. C. F. Millett,[1,a)] G. Whiteman,[1] N. K. Bourne,[1] and G. T. Gray III[2]
[1]*AWE, Aldermaston, Reading, RG7 4PR, United Kingdom*
[2]*MST-8, Los Alamos National Laboratory, Los Alamos, New Mexico 87545, USA*

(Received 30 June 2008; accepted 17 August 2008; published online 9 October 2008)

Manganin stress gauges in lateral orientation have been used to monitor the shock response of Ti–6Al–4V when loaded either parallel to or radial to the long axis of the original bar stock studied in this investigation. Materials characterization has shown that the *c*-axis of the hexagonal unit cell is preferentially orientated radially to the axis of the bar. Shear strengths measured along the long axis of the bar were found to be in agreement with previous data in the literature, while strength in the radial direction was found to be significantly lower. It was also noted that the lateral stress, when measured in the radial direction, displayed a pronounced drop in the lateral stress after reaching the peak shock stress unlike the longitudinal orientation. This decrease is indicative of an increase in shear strength behind the shock front. In both instances, it is postulated that extensive deformation twinning during the early stages of deformation in the shock and thereafter $c+a$ slip and dislocation tangling builds up over a longer time period, resulting in the higher degree of hardening noted. [DOI: 10.1063/1.2991164]

I. INTRODUCTION

The response of the widely used titanium based engineering alloy Ti–6Al–4V (constituents in weight percent—referred henceforth as Ti64) to high rate loading situations has been of interest for a number of years. Primarily this has been driven by the aerospace industry due to its use in aerospace applications such as jet turbine engines. Therefore, it is vulnerable to bird strike and foreign object damage (FOD). More recently, it has also attracted attention as a potential lightweight armor material for military applications. As a consequence, there is a considerable body of work documenting the behavior of this material under impact conditions and the subsequent effect upon mechanical properties. Peters and Ritchie[1] observed that after the impact of a hardened steel sphere onto a flat Ti64 plate in the velocity range of 200–300 m s^{-1}, the fatigue life was reduced by two orders of magnitude. Thompson *et al.*[2] impacted glass spheres onto the leading edges of simulated fan blades, again showing that fatigue life was severely degraded. However, a post impact annealing treatment showed that in some specimens, fatigue performance was restored, suggesting that residual stresses had a major role in the reduction in fatigue response. Reduction in fatigue performance has also been observed to decrease with increasing angle of incidence on the leading edge,[3] although the authors made no direct correlation between impact crater size and loss of fatigue resistance.

At much higher impact velocities (800–1150 m s^{-1}) of interest to the ballistics community, the microstructure of Ti64 has been shown to have a significant effect upon its ballistic performance. Kad and his co-workers[4–6] demonstrated that as annealing temperature increased, ballistic performance was essentially constant, until the beta transus was crossed, whereupon it dropped significantly. Above this level, failure occurred via adiabatic shear banding parallel to the impact axis, resulting in a "clean" plug of the target material of approximately the same diameter as the impactor was removed from the main body of the target. Heat treating below the beta transus resulted in a microstructure where the basal planes of the majority hexagonal close packed (hcp) alpha phase were aligned such that the basal plane normals were orientated toward the long transverse direction of the original rolled plate. Shear localization thus occurred parallel to the rolling direction, hence cracks were oriented parallel to the plate surface. This was due to a combination of the activation of "harder" deformation modes due to the unfavorable orientation of the basal planes and dispersal of the impact energy over a larger area due to the orientation of the cracks. However, the literatures cited above involve complex conditions of strain underneath the impact site, thus rendering a quantitative analysis of the mechanical properties or microstructural development difficult or even impossible. To do so, experiments performed under simpler loading conditions are required. Under quasistatic strain rates, one-dimensional stress can be induced through simple tension or compression, as it also occurs at intermediate strain rates (ca. 10^3 s^{-1}) using the Hopkinson bar. Under shock loading conditions, using plate impact techniques, inertial confinement renders one-dimensional stress nonoperative, but rather, one-dimensional strain conditions prevail.

Ti64 is generally supplied in the α-β condition, essentially a network of hcp α grains, infilled with a small volume fraction of transformed β (very fine grains of α). Deformation is thus dominated by the α grains. The easiest slip system is $\frac{1}{3}\langle 11\bar{2}0\rangle$ on the basal (0001) plane, with slip also occurring on the prismatic $\{1\bar{1}00\}$ and pyramidal $\{1\bar{1}01\}$ planes as well, with little difference between the various critical resolved shear stresses for slip (CRSS).[7] The required $c+a$ $\frac{1}{3}\langle 11\bar{2}3\rangle$ slip has a higher CRSS and occurs on the

a)Electronic mail: jeremy.millett@awe.co.uk.

$\{1\bar{1}01\}$ plane. Under shock loading conditions, Gray and Morris[8] showed that most slip was accommodated with dislocations of Burgers vector $\frac{1}{3}\langle 11\bar{2}0\rangle$. Above 10 GPa, twins of type $\{11\bar{2}1\}$ were also observed. The majority of Ti64 is processed via a casting and hot working route, thus the as-received material exhibits a strongly textured nature dependent on the precise processing route. In unidirectionally rolled plate and bar stock[9] the basal planes in the α phase tend to be orientated toward the long transverse direction of the plate or radial direction of the bar, the effects being more pronounced in plate stock.

Under shock loading conditions, pure titanium undergoes a phase transition from the hcp α phase to the ω phase [possessing a hexagonal structure with a c/a ratio of ca. 0.61 (Ref. 10)] at a pressure of 2.9–9.0 GPa, depending on purity.[11] The ω phase has been shown to be morphologically similar to that produced in as quenched β-phase titanium alloys. However, shock studies on Ti64 in the literature present contradictory findings and interpretations. Rosenberg *et al.*[12] observed a change in slope of the Hugoniot at ca. 10 GPa, while Gray and Morris[8] made no such observations both in terms of the equation of state and transmission electron microscopy analysis of shock recovered samples. The Hugoniot elastic limit (HEL) of Ti64 has been shown by a number of authors[12,13] to lie in the range of 2–3 GPa, depending on microstructure and chemistry. Razorenov *et al.*[14] showed that as oxygen content increased from 0.105 to 0.24 at. %, the HEL increased by 20%, but conversely, the spall (dynamic tensile) strength was unaffected. Others have investigated its spall (shock induced tensile) strength, including Dandekar and Speltzer,[13] Church *et al.*,[15] and Tyler *et al.*[16] showing that spall strength actually increased with pulse duration. The latter authors suggested that damage formation was time dependent, and thus pulse duration would have a strong effect over the tensile behavior.

As has been mentioned previously, Ti64, due to the low symmetry of the hcp unit cell, is anisotropic when processed via conventional routes. While the effect of anisotropy on the mechanical behavior of many metals and alloys has been studied widely under quasistatic strain rates (see for example Smallman[17]), its effects on the shock response of materials is less well documented. In the aluminum alloy 2024, Rosenberg *et al.*[18] noted that the spall strength was greatest when shocked along the rolling direction. Similar results have also been observed for another aluminum alloy 7010-T6,[19] also showing agreement with quasistatic measurements. Additionally, results from 7010-T6 suggested that the short transverse direction was strain rate insensitive, raising the possibility that strain-rate sensitivity itself was orientation dependent. In steels,[20] ballistic performance has been shown to depend on the orientation of manganese sulphide (MnS) stringers (due to processing) to the impact axis. A systematic study on a hot rolled rail steel[21] showed that while the material was crystallographically isotropic (hence showing the HEL to be independent on orientation), the spall strength was lowest in the short transverse direction due to delamination between the MnS stringers and the matrix. Finally, in a cold rolled and annealed zirconium,[22] the quasistatic yield strength was found to be 2.5 times greater in the through thickness direction when compared with that measured in plane. Under shock loading conditions, the dependence of the HEL on orientation agreed with the previous results, although the spall strength was unaffected. Damage evolution *was* affected with the in plane sample showing ductile void growth and the through thickness sample also showing ductile shear cracking.

The shear strength of a material (τ) is defined as the offset of the Hugoniot stress (σ_x) from the hydrostatic pressure P, thus,

$$\sigma_x = P + \frac{4}{3}\tau. \tag{1}$$

If it is assumed that P is the average of the three orthogonal components of stress, shear strength can be written as a function of the longitudinal and lateral stresses (σ_y)

$$2\tau = \sigma_x - \sigma_y. \tag{2}$$

This is a particularly useful parameter as it has been shown to be a good indication of ballistic resistance.[23] By using suitably orientated stress gauges, it is possible to measure both components of stress and thus determine the shear strength.[24,25] Other methods have included calculating the offset of the Hugoniot from the hydrostat, using Eq. (1),[26] using load unload-load reload experiments[27,28] or using transverse displacement interferometry (TDI) during inclined impact.[29] In the case of tungsten and its alloys, it has been possible to compare the results from lateral stress gauges,[30,31] Hugoniot offset,[26] and TDI,[29] showing close agreement between all three techniques, and thus providing confidence in the stress gauge method. An advantage of lateral stress gauges is that by placing them within the material flow during shock loading, it is now able to monitor changes in the shear strength with time behind a shock front. In the case of pure nickel,[32] results showed a decrease in lateral stress, which from Eq. (2) indicated an increase in shear strength behind the shock front. This appeared to correlate with the early work of Murr and Kuhlmann–Wilsdorf,[33] who, in making recovery experiments, showed that the dislocation cell structure in shocked nickel required between 0.5 and 1 μs to reach its equilibrium state. In contrast, tantalum has been shown to *increase* its lateral stress behind the shock front,[34] thus showing a *decrease* in shear strength. This was explained in terms of the high Peierl's (lattice friction) stress restricting dislocation generation in tantalum, but rather largely depending more on the motion of pre-existing dislocations. As the initial dislocation density (ρ) was quite low and the imposed strain-rate ($\dot{\gamma}$) was very high due to the shock front, the resultant dislocation velocity v would also have to be high through Orowan's relation

$$\dot{\gamma} = b\rho v, \tag{3}$$

where b is the Burgers vector. A high dislocation velocity requires high stresses to drive deformation. However, as dislocation density increases during the later stages of deformation and assuming that the strain rate remains constant, dislocation velocity drops, and thus the shear strength will also decrease. Similar results have additionally been observed in

pure tungsten[31] and a tungsten heavy alloy (WHA).[30] In the case of pure tungsten, it was also suggested that a degree of brittle cracking may have also contributed to the reduction in shear strength behind the shock front.

In the case of Ti64, lateral stress measurements made by Hopkins and Brar[35] showed an increase in shear strength with impact stress. Their results also suggested that there was a small reduction in lateral stress behind the shock front, but as the authors did not quantify in the paper the chemistry, microstructure, or texture of their material studied, it is difficult to make detailed comments or comparisons.

In the current study, we report lateral stress measurements in a Ti64 material of known pedigree. We have also characterized the microstructure as a function of orientation to the original bar stock directions and have thus measured the shear strength as a function of both applied shock stress and orientation, (i.e., crystallographic texture) to the bar stock.

II. EXPERIMENTAL

All shots were performed on a 3 m long, 70 mm bore single stage gas gun. Ti64 shock samples were machined from the original bar stock such that the impact axis was either parallel to or radial to the long axis of the billet. Each sample was 8 mm thick by 50×50 mm^2. The samples were further sectioned in half and a manganin stress gauge (MicroMeasurements type J2M-SS-380SF-025) was introduced 4 mm from the front surface. In this orientation, the gauge would be sensitive to the lateral component of stress. The specimen plate was reassembled using a low viscosity adhesive and held in a special jig for a minimum of 12 h. Afterward, the front surface was lapped such that it was flat to within five fringes from a monochromatic light source. Stress data were determined from the voltage data using the methods of Rosenberg and Partom[25] using a modified analysis that does not require prior knowledge of the impact conditions.[36] Finally, in a very recent paper, we also showed that the geometry of the gauge itself can effect the results at low stresses, which must be accounted for.[37] The shock sample was then fixed to a 3 mm driver plate of either dural (aluminum alloy 6082-T6) or copper matched to the material of the flyer plate. In some cases, another manganin stress gauge (LM-SS-125CH-048) was placed between the two, such that the Hugoniot could be determined. The gauges were calibrated according to Rosenberg *et al.*[38] Gauge placements and target assemblies are shown schematically below in Fig. 1.

Impact stresses in the range of 4.4–10 GPa were generated through impacting with 6 mm thick flyer plates of either Dural (aluminum alloy 6082-T6) or copper, both of whose impact responses are well understood,[39] at velocities of 461–654 m s^{-1}. Acoustic properties were measured in both the longitudinal and radial orientations using ultrasonic transducers at a frequency of 5 MHz.

III. MATERIALS' DATA

The Ti64 studied was supplied as hot rolled and annealed at 75 mm bar stock. The chemical composition was (weight percent) Al 6.46, V 4.04, Fe 0.16, C 0.01, O 0.18, N 0.0055, H 0.0035, and balanced Ti. The material was shown to possess a $\langle 10\bar{1}0 \rangle$ rod axial fiber direction texture of moderate strength (ca. $\times 4$). The mechanical properties in the longitudinal direction (as supplied by the manufacturers) were 0.2% proof stress=874 MPa, tensile strength =963 MPa, and the tensile elongation=20.5%. The grain size was ASTM 10. The acoustic properties for both orientations are shown in Table I.

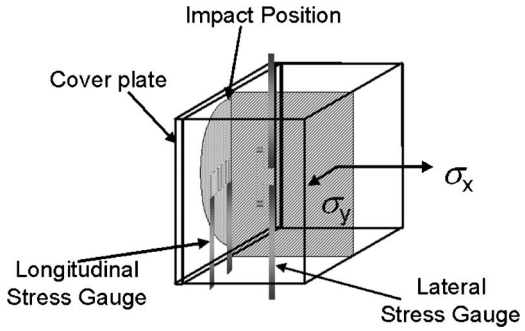

FIG. 1. Specimen configuration and gauge placement.

A representative pole figure and the as-received microstructure are shown in Fig. 2.

IV. RESULTS

In Fig. 3, we present typical results from Ti64 using both longitudinal and lateral stress gauges. The impact conditions were that of a 5 mm copper flyer plate at 454 m s^{-1}.

Note that the longitudinal gauge (labeled σ_x), as it was mounted on the copper/Ti-6Al-4V interface, only provided the impact stress and through conservation of momentum, the particle (material flow behind the shock front) velocity, u_p, which is discussed later in the text. The lateral stress gauge mounted 4 mm into the target is more informative as the shock pulse will have been modified as it passed through the sample material. Note that the lateral stress rises to a peak value of ca. 5.0 GPa, before decreasing slightly over a period of 0.5 μs before reaching a constant value of nominally 4.8 GPa. The longitudinal gauge trace was used to generate Hugoniot data, which was compared with the existing Hugoniots reported by Rosenberg *et al.*,[12] Gray and Morris,[8] and Hopkins and Brar.[35] This Hugoniot comparison for Ti64 is presented below in Fig. 4.

As with the current data, Rosenberg *et al.*[12] and Hopkins and Brar[35] used manganin stress gauges, while Gray and Morris[8] determined the particle velocity using velocity interferometry using any reflector (VISAR). Observe that there is close agreement, both between all three sets of gauge data

TABLE I. Acoustic properties in Ti–6Al–4V.

Orientation	ρ_0 g/cm^3	c_L mm/μs	c_S mm/μs	υ
Longitudinal	4.4	6.11	3.13	0.322
Radial	4.4	6.18	3.18	0.320

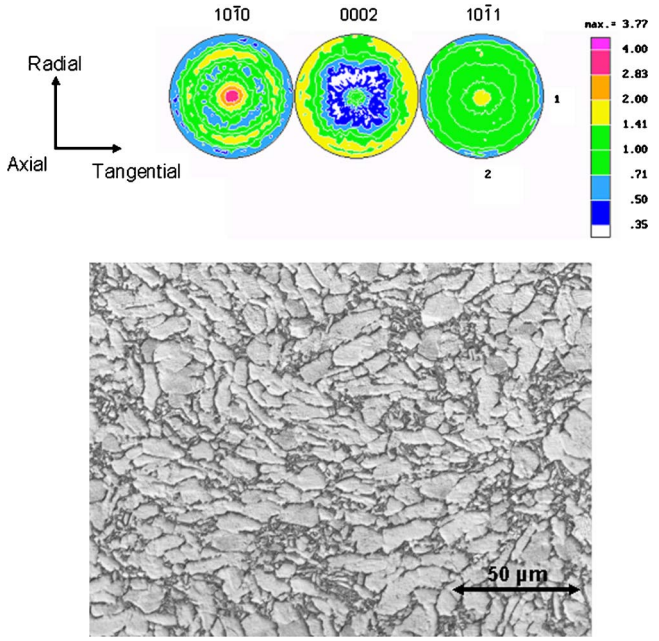

FIG. 2. (Color online) Microstructure and orientation of the as-received material. (a) α-phase pole figures for the $[10\bar{1}0]$, [0002], and $[10\bar{1}1]$ directions. Measurements were taken from the central position along the long axis of the billet. (b) As-received microstructure. The long axis of the billet is in the vertical direction.

and the VISAR data, which has been used to calculate the hydrodynamic pressure P_{HD} through the relation

$$P_{HD} = \rho_0(c_0 + Su_p)u_p, \tag{4}$$

where ρ_0 is the ambient density and c_0 and S (the shock parameters) are 5.12 mm μs^{-1} and 1.08, respectively.[8] This is unsurprising as the Hugoniots of many pure metals and their simple alloys, in terms of stress and particle velocity, have been observed to be essentially identical in stress terms. Examples include iron and mild steel,[40] tungsten and WHAs,[30] and nickel and nickel −60 wt % cobalt.[32] More significantly, it can be concluded that from the degree of scatter of the gauge data, there is little or no difference in the equation of state of Ti64 due to orientation of loading axis. This similarity provides us with confidence that subsequent measurements of the shear strength, based on the existing data for the Hugoniot of Ti64, are correct.

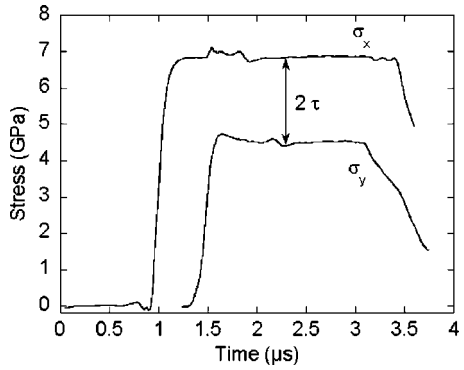

FIG. 3. Typical longitudinal and lateral stress gauge traces for shock loaded Ti64. The specimen was shocked along the longitudinal bar axis with a 5 mm copper flyer at 454 m s^{-1}.

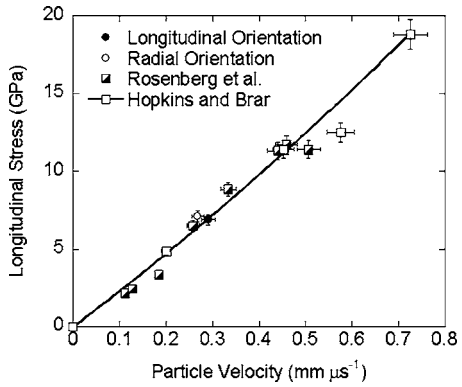

FIG. 4. Hugoniot of Ti64 in stress-particle velocity space. The curve fit is according to Eq. (4) using the data of Gray and Morris (Ref. 8).

In Fig. 5, we compare lateral stress traces for the current Ti64 for both shock-loading orientations taken under near identical impact conditions (9.85 GPa for the longitudinal and 9.40 GPa for the radial orientation).

In this example, clear differences can be observed between the two loading orientations. In the longitudinal direction, the lateral stress is seen to be nearly flat behind the shock front, indicating that the shear strength is also constant. In contrast, the radial orientation displays a marked decrease in lateral stress, corresponding to an increase in the shear strength. This is a first indication that the shear strength of this material is orientation dependent. This is likely affected by the alignment of the various slip and deformation twinning systems activated relative to the imposed loading axis during shock loading.

Finally, in Fig. 6, we have plotted the calculated shear strengths [using Eq. (2)] against the longitudinal stress. We have also included the corresponding data of Hopkins and Brar[35] for comparison. In all cases, we have used the lateral stress immediately behind the shock front to calculate the shear strength, as indicated by the left-hand arrow on the radially orientated trace in Fig. 5.

The straight line is the calculated elastic response according to

$$2\tau = \frac{1-2\nu}{1-\nu}\sigma_x. \tag{5}$$

In the case of our longitudinally orientated data, as well as that of Hopkins and Brar,[35] there is a clear agreement, while

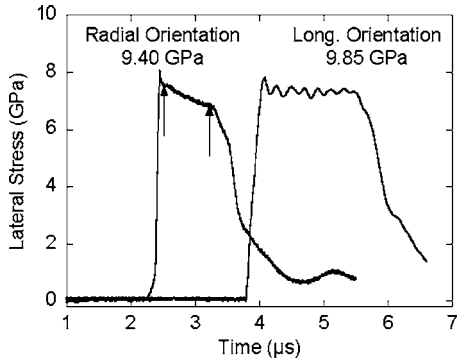

FIG. 5. Lateral stress gauge traces in Ti64 from the longitudinal and radial orientations.

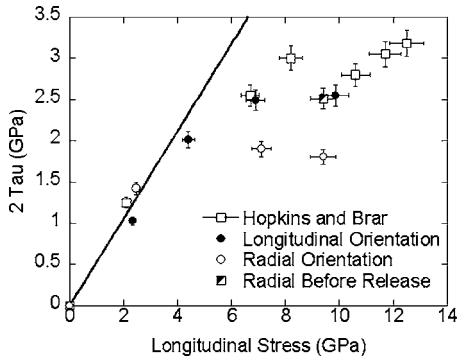

FIG. 6. Shear strength vs longitudinal stress for Ti64.

the radially orientated specimens show a considerable reduction in shear strength. However, from Fig. 5, we have also measured the lateral stress just before the arrival of the release at the gauge location in one radially orientated sample. This has been used to determine the shear strength at that time and is included in Fig. 6, labeled as "radial before release." Observe that the shear strength in this sample has increased to where it is essentially coincident with the shear strength of the longitudinally orientated samples. This suggests that while the early stages of deformation in the shock appear strongly influenced by the anisotropy in Ti64, at later stages, conditions seem to equalize.

V. DISCUSSION

The motivation behind this investigation was to study the effects of material anisotropy on the shock induced mechanical behavior of Ti64. We have done so using lateral stress gauges as this allows us to monitor the shear strength and the way it changes with pulse duration behind the shock front. We also wanted to quantify if anisotropy may also manifest itself in the Hugoniot, although the Hugoniot itself has been determined by a number of authors,[8,12,35] results showing that there is a close agreement between all sets of data. Although we ourselves only made a limited number of measurements, we did so longitudinally and radially to the long axis of a textured Ti64 billet. In doing so, we showed that not only did our own data agree with that published previously in the literature, but that there were no significant differences between orientations in terms of the Hugoniot. These results were expected as Hugoniot measurements in metals and their alloy systems, such as nickel[32] and tungsten,[31] have been shown to be nearly identical.

The major difference in orientation were found in the shear strength, both in its absolute variation with impact stress and its local variation behind the shock front. First, from Fig. 6, it is clear that the shear strength of Ti64 when shocked along the longitudinal orientation is considerably higher than when shocked in the radial direction. Given the texture of the original bar stock, with the $\langle 10\bar{1}0\rangle$ direction preferentially orientated along the long axis of the bar stock, these results would seem at first unexpected. As a consequence, when shocked radially, there will be a greater requirement for $c+a$ dislocations and/or compressive deformation twinning to accommodate the imposed shock deformation, which since they have a greater CRSS would lead one to expect a higher shear strength. However, a possible explanation occurs if one considers deformation twinning in addition to the potential operative slip systems. In a previous investigation on nickel alloys,[41] it was noted that the shear strength of pure nickel was considerably higher than that of the alloy, Ni–60Co, when one might expect the opposite situation to apply, given the solid-solution hardening in the Ni–60Co alloy. A simple examination of the shocked microstructures showed that the alloy relied heavily on twin formation to accommodate the imposed deformation. Further, Rohatgi *et al.*,[42,43] in their investigation of Cu–Al alloys, showed that the postshock prestrained shock hardening of recovered samples reduced as aluminum content increased, stacking fault energy decreased, and hence twin formation increased. This would suggest that twins themselves, while capable of rapidly relieving the applied shear stresses, actually contribute less to the overall strain hardening, and therefore the strength during shock loading, and with less strain hardening, less postshock hardening in shock recovered samples. Although we did not recover any of the Ti64 samples in the current investigation for microstructural analysis, the referenced works above support the concept that the lower strengths exhibited by samples shocked in the radial direction are due to a combination of initially rapid twin activation followed by $c+a$ slip and through tangling with these twins strain hardening. Here, we propose that although the radial direction is notionally harder to deform based on purely slip activation, the requirement for dislocations with a $c+a$ component to form may encourage deformation to have a significant twinning contribution. Previous work by Gray and Morris[8] documented that shock prestrained Ti64 displayed twin formation, however, that study did not address the effects of anisotropy on strength in the shock. Assuming that twin formation is favored when shock is loaded along the radial orientation, this would be consistent with the observation that the measured shear strength should be lower than the longitudinal orientation.

The final point as regards the shear stress data is the *shape* of the lateral stress histories. From Fig. 5, it can be seen that the radially orientated trace shows a much greater decrease behind the shock front than its longitudinally orientated counterpart. In a previous article,[41] we proposed that the mobility of dislocations and ability to generate and store new dislocation line length affected the nature of material flow, and hence the shape of the lateral stress history behind the shock front in nickel and its alloys. More specifically in that investigation, it was proposed that decreasing stacking fault energy (SFE), resulting in a wider separation of partial dislocations, reduced overall dislocation mobility with some of that imposed deformation accommodated via twin formation. In particular, from the analysis of the spall response, where it was noted that in pure nickel (high SFE) where deformation is dislocation dominated, the spall strength appeared essentially constant with pulse duration. In contrast, in Ni–60Co (low SFE), spall strength was observed to increase with pulse duration. In the case of shear strength measurements (using lateral stress gauges), nickel was observed to have a small degree of hardening, while in Ni–60Co, the

degree of hardening was much greater. This also correlates with the observations of Rohatgi *et al.*[42,43] that twinning had little overall contribution to any shock induced hardening and led us to propose that in nickel alloys,[41] twinning occurred in the very early stages of deformation but did not significantly contribute to the overall hardening. In the case of Ti64, it is suggested that a similar mechanism is in operation, in this case due to the ease of dislocation generation and motion and the effects of orientation. With the majority of the basal plane normals orientated radially within the original billet, dislocation dominated deformation will be easier when shocked along the long axis of the billet. In contrast, deformation in the radial direction would be more likely to initially involve rapid twin activation followed by $c+a$ slip and through dislocation tangling and slip-twinning interactions strain hardening consistent with the increasing shear strength in the radially shocked orientation.

VI. CONCLUSIONS

A series of plate impact experiments has been performed to quantify the role of anisotropy on the response of the titanium alloy Ti–6Al–4V to shock loading. Specifically, this has involved the use of manganin stress gauges mounted such that they are sensitive to the lateral component of stress, and hence can be used to determine the shock induced shear strength. Prior material characterization has shown that the Ti64 used in this investigation has a moderate rod axial $\langle 10\bar{1}0\rangle$ fiber texture (approximately four times random). A limited number of Hugoniot stress measurements have shown that the equation of state of this Ti64 when shocked in either the longitudinal or radial direction is in good agreement with similar measurements in the literature. The shear strength measurements are more illuminating. When shocked in the longitudinal orientation, shear strengths have been shown to agree with the work of others with a limited degree of hardening behind the shock front. In the radial orientation, the initial shear strength (immediately behind the shock front) has been shown to be lower than the longitudinal orientation. We believe that the unfavorable orientation of the unit cell in the radial direction favors early twin formation during the shock rise, which results in an initially reduced shear strength. In a similar way, the prevalence of twin formation in the radial direction delays dislocation generation and motion, and hence results in the greater degree of change in shear strength behind the shock front via $c+a$ slip and strain hardening.

As aerospace components manufactured by thermomechanical processing will be anisotropic in nature, it is vital that this be incorporated into physics based models if impact events such as bird strike and FOD are to be successfully predicted. The data presented in this article, while highly idealized in the loading geometry, nevertheless provide basic input data for such models.

ACKNOWLEDGMENTS

We would like to thank Peter Keightley, Mike Lowe and Alex Mole of AWE, and John Bingert and Ellen Cerreta of Los Alamos National Laboratories for their help in this program. British Crown Copyright MOD/2008.

[1] J. O. Peters and R. O. Ritchie, Eng. Fract. Mech. **67**, 193 (2000).
[2] S. R. Thompson, J. J. Ruschau, and T. Nicholas, Int. J. Fatigue **23**, 405 (2001).
[3] J. J. Ruschau, T. Nicholas, and S. R. Thompson, Int. J. Impact Eng. **25**, 233 (2001).
[4] B. K. Kad, S. E. Schoenfeld, and M. S. Burkins, Metall. Mater. Trans. A **33A**, 937 (2002).
[5] S. E. Schoenfeld and B. K. Kad, Int. J. Plast. **18**, 461 (2002).
[6] B. K. Kad, S. E. Schoenfeld, and M. S. Burkins, Mater. Sci. Eng., A **322**, 241 (2002).
[7] I. P. Jones and W. B. Hutchinson, Acta Metall. **29**, 951 (1981).
[8] G. T. Gray III and C. E. Morris, Sixth World Conference on Titanium, France, 1988 (unpublished), pp. 269–274.
[9] D. S. McDarmaid and P. G. Partridge, J. Mater. Sci. **21**, 1525 (1986).
[10] E. Cerreta, G. T. Gray III, A. C. Lawson, T. A. Mason, and C. E. Morris, J. Appl. Phys. **100**, 013530 (2006).
[11] C. W. Greeff, D. R. Trinkle, and R. C. Albers, J. Appl. Phys. **90**, 2221 (2001).
[12] Z. Rosenberg, Y. Meybar, and D. Yaziv, J. Phys. D **14**, 261 (1981).
[13] D. P. Dandekar and S. V. Spletzer, in *Shock Compression of Condensed Matter 1999*, edited by M. D. Furnish, L. C. Chhabildas, and R. S. Hixson (AIP, Melville, NY, 2000), pp. 427–430.
[14] S. V. Razorenov, G. I. Kanel, A. V. Utkin, A. A. Bogach, M. Burkins, and W. A. Gooch, in *Shock Compression of Condensed Matter-1999*, edited by M. D. Furnish, L. C. Chhabildas, and R. S. Hixson (AIP, Melville, NY, 2000), pp. 415–418.
[15] P. D. Church, T. Andrews, N. K. Bourne, and J. C. F. Millett, in *Shock Compression of Condensed Matter-2001*, edited by M. D. Furnish, N. Thadhani, and Y. Horie (AIP, Melville, NY, 2002), pp. 511–514.
[16] C. Tyler, J. C. F. Millett, and N. K. Bourne, in *Shock Compression of Condensed Matter-2005*, edited by M. D. Furnish (AIP, Melville, NY, 2006), pp. 674–677.
[17] R. E. Smallman, *Modern Physical Metallurgy* (Butterworths, London, 1985).
[18] Z. Rosenberg, G. Luttwak, Y. Yeshurun, and Y. Partom, J. Appl. Phys. **54**, 2157 (1983).
[19] R. Vignjevic, N. K. Bourne, J. C. F. Millett, and T. de Vuyst, J. Appl. Phys. **92**, 4342 (2002).
[20] P. W. Leach and R. L. Woodward, J. Mater. Sci. **20**, 854 (1985).
[21] G. T. Gray III, N. K. Bourne, J. C. F. Millett, M. F. Lopez, and K. S. Vecchio, in *Shock Compression of Condensed Matter-2001*, edited by M. D. Furnish, N. Thadhani, and Y. Horie (AIP, Melville, NY, 2002), pp. 479–482.
[22] G. T. Gray III, N. K. Bourne, M. A. Zocher, P. J. Maudlin, and J. C. F. Millett, in *Shock Compression of Condensed Matter-1999*, edited by M. D. Furnish, L. C. Chhabildas, and R. S. Hixson (AIP, Woodbury, NY, 2000), pp. 509–512.
[23] L. W. Meyer, F. J. Behler, K. Frank, and L. S. Magness, Proceedings of the 12th International Symposium Ballistics, San Antonio, TX, 1990 (unpublished), pp. 419–428.
[24] Y. M. Gupta, D. D. Keough, D. Henley, and D. F. Walter, Appl. Phys. Lett. **37**, 395 (1980).
[25] Z. Rosenberg and Y. Partom, J. Appl. Phys. **58**, 3072 (1985).
[26] D. P. Dandekar and W. J. Weisgerber, Int. J. Plast. **15**, 1291 (1999).
[27] J. Lipkin and J. R. Asay, J. Appl. Phys. **48**, 182 (1977).
[28] H. Huang and J. R. Asay, J. Appl. Phys. **98**, 033524 (2005).
[29] M. Zhou and R. J. Clifton, J. Appl. Mech. **64**, 487 (1997).
[30] J. C. F. Millett, N. K. Bourne, Z. Rosenberg, and J. E. Field, J. Appl. Phys. **86**, 6707 (1999).
[31] J. C. F. Millett, G. T. Gray III, and N. K. Bourne, J. Appl. Phys. **101**, 033520 (2007).
[32] J. C. F. Millett, Y. J. E. Meziere, and N. K. Bourne, J. Mater. Sci. **42**, 5941 (2007).
[33] L. E. Murr and D. Kuhlmann-Wilsdorf, Acta Metall. **26**, 847 (1978).
[34] G. T. Gray III, N. K. Bourne, and J. C. F. Millett, J. Appl. Phys. **94**, 6430 (2003).

[35]A. Hopkins and N. S. Brar, in *Shock Compression of Condensed Matter 1999*, edited by M. D. Furnish, L. C. Chhabildas, and R. S. Hixson (AIP, Melville, NY, 2000), pp. 423–426.
[36]J. C. F. Millett, N. K. Bourne, and Z. Rosenberg, J. Phys. D **29**, 2466 (1996).
[37]Z. Rosenberg, N. K. Bourne, and J. C. F. Millett, Meas. Sci. Technol. **18**, 1843 (2007).
[38]Z. Rosenberg, D. Yaziv, and Y. Partom, J. Appl. Phys. **51**, 3702 (1980).
[39]S. P. Marsh, *Shock Hugoniot Data* (University of California, Los Angeles, 1980).
[40]N. Bourne and J. Millett, Scr. Mater. **43**, 541 (2000).
[41]J. C. F. Millett, N. K. Bourne, and G. T. Gray III, Metall. Mater. Trans. A **39**, 322 (2008).
[42]A. Rohatgi, K. S. Vecchio, and G. T. Gray III, Metall. Mater. Trans. A **32**, 135 (2001).
[43]A. Rohatgi, K. S. Vecchio, and G. T. Gray III, Acta Mater. **49**, 427 (2001).